Broken-axisymmetry phase of a spin-1 ferromagnetic Bose-Einstein condensate

Keiji Murata,[1] Hiroki Saito,[2] and Masahito Ueda[1,3]
[1]*Department of Physics, Tokyo Institute of Technology, Tokyo 152-8551, Japan*
[2]*Department of Applied Physics and Chemistry, The University of Electro-Communications, Tokyo 182-8585, Japan*
[3]*ERATO, Japan Science and Technology Corporation (JST), Saitama 332-0012, Japan*
(Received 7 July 2006; published 5 January 2007)

A spin-1 ferromagnetic Bose-Einstein condensate subject to a certain magnetic field exhibits a broken-axisymmetry phase in which the magnetization tilts against the applied magnetic field due to the competition between ferromagnetism and linear and quadratic Zeeman effects. The Bogoliubov analysis shows that in this phase two Goldstone modes associated with U(1) and SO(2) symmetry breakings exist, in which phonons and magnons are coupled to restore the two broken symmetries.

DOI: 10.1103/PhysRevA.75.013607 PACS number(s): 03.75.Mn, 67.40.Db, 67.57.Jj

I. INTRODUCTION

Bose-Einstein condensates (BECs) with spin degrees of freedom have attracted growing attention since the first observation of the spin-1 ^{23}Na BEC by the MIT group [1,2]. In contrast to a magnetic trap, in which hyperfine-spin degrees of freedom are frozen, an optical trap can confine atoms in all magnetic sublevels of spin, allowing study of the magnetic properties of BECs. A variety of experiments have been performed to date, on subjects such as spin domains [3], interdomain tunneling [4], and realization of a spin-2 ^{23}Na BEC [5]. The spin-exchange dynamics of ^{87}Rb BECs have also been investigated experimentally by Schmaljohann *et al.* [6], Chang *et al.* [7], and Kuwamoto *et al.* [8].

Extensive theoretical investigations have been focused on the spinor BEC. Mean field theory (MFT) for a spin-1 BEC was formulated by Ho [9] and Ohmi and Machida [10]. The MFT of a spin-2 BEC was developed by Ciobanu *et al.* [11] and Ueda and Koashi [12]. Law *et al.* [13] developed a many-body theory of spin-1 antiferromagnetic BEC, and Koashi and Ueda [14] and Ho and Yip [15] extended it to including the linear Zeeman effect and found that an antiferromagnetic BEC realizes a fragmented BEC for a very weak magnetic field. The Bogoliubov analysis of a spin-1 BEC was carried out by Huang and Gou [16] and by Ueda [17] in the presence of the linear Zeeman effect. Their results agree with those obtained later using a diagrammatic method reported by Szépfalusy and Szirmai [18]. In these studies, the Zeeman effects are restricted to those up to the linear order in the magnetic field. Since the linear Zeeman effect can be effectively tuned by changing the total spin of the system [2], the linear and quadratic Zeeman effects can be manipulated independently, which is a unique feature of trapped atomic systems. If we take the quadratic Zeeman term into account, the ground-state phase diagram becomes much richer, as shown in Ref. [2]. In particular, under a certain range of linear and quadratic Zeeman effects, there is a special phase in which the magnetization tilts against the applied magnetic field. The investigation of some of the unique features of this phase is the primary purpose of our study.

When a weak magnetic field is applied along the quantization axis, the $m=1$ or -1 state is favorable for a spin-1 ^{87}Rb atom depending on the sign of the magnetic field, where m refers to the magnetic quantum number. On the other hand, the quadratic Zeeman effect raises the energy of the $m=\pm 1$ states relative to that of the $m=0$ state. As a consequence, if the quadratic Zeeman effect is sufficiently large, the spin vector of the ferromagnetic ground state not only shrinks but also tilts against the direction of the magnetic field. Therefore, even if the Hamiltonian is axisymmetric with respect to the direction of the magnetic field, the ground state spontaneously breaks the axisymmetry. This phase, which we shall refer to as the broken-axisymmetry phase, was predicted in Ref. [2], but little attention has been paid to it from the viewpoint of symmetry breaking. Recently, the spontaneous axisymmetry breaking in this phase was observed in the magnetization dynamics of a spin-1 ^{87}Rb BEC by the Berkeley group [19].

In the present study, we investigate the Goldstone modes of this phase by studying its excitation spectrum. The BEC with ferromagnetic interactions has three phases: ferromagnetic, polar, and broken-axisymmetry phases. In the ferromagnetic and polar phases, only the U(1) (global phase) symmetry is broken, and the associated Goldstone mode is a phonon. In the broken-axisymmetry phase, the SO(2) symmetry (axisymmetry) of the spin vector is broken in addition to the U(1) symmetry. Because of the simultaneous breaking of these two continuous symmetries, the associated Goldstone modes are expected to involve both phonons and magnons.

This paper is organized as follows. Section II reviews the mean-field ground state of a spin-1 BEC to make this paper self-contained. Section III uses the Bogoliubov theory to derive one gapful mode and two gapless Goldstone modes. Section IV explores the implications of the present study for other related studies, and Sec. V concludes this paper. Appendix A derives analytic expressions for the ground-state spinor and magnetization of the broken-axisymmetry phase. Appendix B discusses the excitation spectra of the ferromagnetic and polar phases for comparison with the excitation spectrum of the broken-axisymmetry phase.

II. GROUND STATE WITH BROKEN AXISYMMETRY

A. Formulation of the problem

We consider a uniform system of N identical bosons with hyperfine spin 1 in which an external magnetic field is ap-

plied in the z direction. The Hamiltonian of the system is written as the sum of one-body part $\hat{\mathcal{H}}_{\mathrm{I}}$ and two-body interaction part $\hat{\mathcal{H}}_{\mathrm{II}}$. The one-body part is given by

$$\hat{\mathcal{H}}_{\mathrm{I}} = \sum_{m=-1}^{1} \int d\mathbf{r}\, \hat{\Psi}_m^{\dagger} \left(-\frac{\hbar^2}{2M}\nabla^2 - pm + qm^2 \right) \hat{\Psi}_m, \quad (1)$$

where subscripts $m=+1, 0, -1$ denote the magnetic quantum numbers along the z axis and M is the mass of the atom. The coefficient p is the sum of the linear Zeeman energy and the Lagrange multiplier [2] and q is the quadratic Zeeman energy. The Lagrange multiplier is introduced to set the total magnetization in the z direction to a prescribed value, which is conserved due to the axisymmetry of the system. In the cases of spin-1 ^{23}Na and ^{87}Rb atoms, q is positive. The two-body part, which is described by a contact-type s-wave interaction at ultralow temperature, takes the form

$$\hat{\mathcal{H}}_{\mathrm{II}} = \frac{1}{2}\sum_{F=0,2} g_F \int d\mathbf{r}\, \hat{\Psi}_{n'}^{\dagger}\hat{\Psi}_{m'}^{\dagger}\langle m';n'|\mathcal{P}_F|m;n\rangle \hat{\Psi}_m \hat{\Psi}_n, \quad (2)$$

where $g_F = 4\pi\hbar^2 a_F/M$ with a_0 and a_2 being the s-wave scattering lengths in the singlet and quintuplet channels, respectively, and $\mathcal{P}_F$ projects a two-body state into that with total spin F. The projection onto the $F=1$ channel is absent due to the Bose statistics.

Because the system is uniform, it is convenient to work in the momentum space by expanding the field operators in terms of plane waves as $\hat{\Psi}_m = \Omega^{-1/2}\Sigma_{\mathbf{q}} e^{i\mathbf{q}\cdot\mathbf{r}}\hat{a}_{\mathbf{q},m}$, where Ω is the volume of the system and $\hat{a}_{\mathbf{q},m}$ represents the annihilation operator of a boson with wave number $\mathbf{q}$ and magnetic quantum number m. Equations (1) and (2) are then rewritten as

$$\hat{\mathcal{H}}_{\mathrm{I}} = \sum_{\mathbf{k},m} (\epsilon_{\mathbf{k}} - pm + qm^2)\hat{a}_{\mathbf{k},m}^{\dagger}\hat{a}_{\mathbf{k},m}, \quad (3)$$

$$\hat{\mathcal{H}}_{\mathrm{II}} = \frac{c_0}{2\Omega}\sum_{\mathbf{k}} :\hat{\rho}_{\mathbf{k}}^{\dagger}\hat{\rho}_{\mathbf{k}}: + \frac{c_1}{2\Omega}\sum_{\mathbf{k}} :\hat{\mathbf{f}}_{\mathbf{k}}^{\dagger}\cdot\hat{\mathbf{f}}_{\mathbf{k}}:, \quad (4)$$

where $\epsilon_{\mathbf{k}} = \hbar^2\mathbf{k}^2/(2M)$, $c_0 = (g_0+2g_2)/3$, $c_1 = (g_2-g_0)/3$, $\hat{\rho}_{\mathbf{k}} = \Sigma_{\mathbf{q},m}\hat{a}_{\mathbf{q},m}^{\dagger}\hat{a}_{\mathbf{q}+\mathbf{k},m}$, and $\hat{\mathbf{f}}_{\mathbf{k}} = \Sigma_{\mathbf{q},m,n}\mathbf{f}_{m,n}\hat{a}_{\mathbf{q},m}^{\dagger}\hat{a}_{\mathbf{q}+\mathbf{k},n}$ with $\mathbf{f} = (f_x, f_y, f_z)$ being the spin-1 matrices in vector notation [see Eq. (A13)]. The symbol $::$ denotes the normal ordering of operators. The spin-spin interaction is ferromagnetic if $c_1 < 0$ and antiferromagnetic if $c_1 > 0$. It is known that the interaction between spin-1 ^{23}Na atoms is antiferromagnetic and that between spin-1 ^{87}Rb atoms is ferromagnetic [20,21].

Assuming that a macroscopic number of atoms occupy the $\mathbf{k}=\mathbf{0}$ state, we replace the relevant operators with c numbers. The Hamiltonian for the BEC in the $\mathbf{k}=\mathbf{0}$ state is given by

$$\hat{\mathcal{H}}_{\mathrm{BEC}} = \frac{c_0}{2\Omega}:\left(\sum_{m=-1}^{1}\hat{a}_{\mathbf{0},m}^{\dagger}\hat{a}_{\mathbf{0},m}\right)^2: + \sum_{m=-1}^{1}(-pm+qm^2)\hat{a}_{\mathbf{0},m}^{\dagger}\hat{a}_{\mathbf{0},m} - \frac{c_1}{2\Omega}\hat{s}^{\dagger}\hat{s}, \quad (5)$$

where

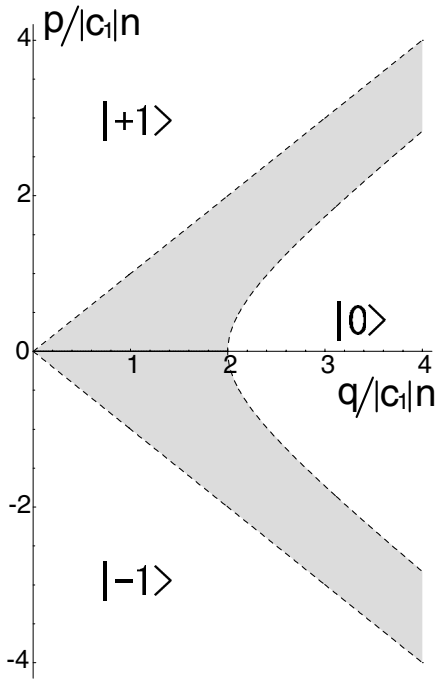

FIG. 1. Ground-state phase diagram for a spin-1 ferromagnetic BEC, where $|c_1|n$ is the ferromagnetic interaction energy, p is the sum of the linear Zeeman energy and the Lagrange multiplier that determines the total magnetization in the z direction, and q is the quadratic Zeeman energy. The dashed curves indicate second-order phase boundaries. In the figure, $|+1\rangle$ and $|-1\rangle$ represent the ferromagnetic phase and $|0\rangle$ represents the polar phase. The shaded region is the broken-axisymmetry phase, in which the magnetization tilts against the z axis.

$$\hat{s} = \frac{1}{\sqrt{3}}(\hat{a}_{\mathbf{0},0}^2 - 2\hat{a}_{\mathbf{0},1}\hat{a}_{\mathbf{0},-1}) \quad (6)$$

is an annihilation operator for a singlet pair. In the MFT, we replace the operator $\hat{a}_{\mathbf{0},m}$ with c-number $\zeta_m\sqrt{N_0}$. Here N_0 is the number of condensed atoms and the order parameters ζ_m's are complex variational parameters that are determined so as to minimize the energy functional under the constraint of normalization $\Sigma_m|\zeta_m|^2 = 1$. For this purpose, we introduce a Lagrange multiplier μ and minimize $\langle\mathcal{H}\rangle - \mu N_0\Sigma_m|\zeta_m|^2$ with respect to $\boldsymbol{\zeta}_m$. In the following, we denote the set of the order parameters as $\boldsymbol{\zeta} = {}^T(\zeta_1, \zeta_0, \zeta_{-1})$, where the superscript T stands for transpose.

B. Ground states

The ground-state phase diagram for a spin-1 ferromagnetic BEC is shown in Fig. 1 [2]. The phases are classified as follows.

(1) Ferromagnetic phase ($|+1\rangle$ and $|-1\rangle$ in Fig. 1). The order parameter is given for $p>0$ by $\boldsymbol{\zeta}_F = {}^T(e^{i\chi_1}, 0, 0)$ and for $p<0$ by $\boldsymbol{\zeta}_F = {}^T(0, 0, e^{i\chi_{-1}})$, where χ_m denotes an arbitrary phase of ζ_m, i.e., $\zeta_m = |\zeta_m|e^{i\chi_m}$.

(2) Polar phase ($|0\rangle$ in Fig. 1). The order parameter is given by $\boldsymbol{\zeta}_P = {}^T(0, e^{i\chi_0}, 0)$.

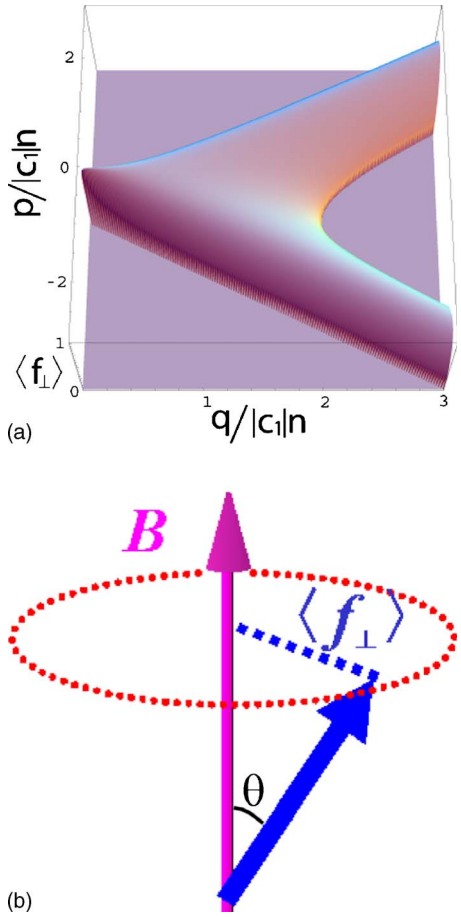

FIG. 2. (Color online) (a) Transverse magnetization, i.e., magnetization perpendicular to the direction of the applied magnetic field $\langle f_\perp\rangle \equiv \langle F_\perp\rangle/N_0$ as a function of linear and quadratic Zeeman coefficients. The transverse magnetization is nonzero only in the broken-axisymmetry phase. (b) Schematic illustration of the spin vector in the broken-axisymmetry phase.

(3) Broken-axisymmetry phase (shaded region in Fig. 1). The order parameter is given by (see Appendix A for derivation)

$$\zeta_{\pm 1} = (q \pm p)\sqrt{\frac{p^2 + 2|c_1|nq - q^2}{8|c_1|nq^3}}e^{i\chi_{\pm 1}},$$

$$\zeta_0 = \sqrt{\frac{(q^2 - p^2)(p^2 + 2|c_1|nq + q^2)}{4|c_1|nq^3}}e^{i(\chi_1+\chi_{-1})/2}. \tag{7}$$

In the broken-axisymmetry phase, the transverse magnetization, which is perpendicular to the external magnetic field [see Fig. 2(b)], is nonzero and given by

$$\langle F_\perp\rangle \equiv \sqrt{\langle F_x\rangle^2 + \langle F_y\rangle^2} = N_0\frac{\sqrt{q^2 - p^2}\sqrt{(p^2 + 2|c_1|nq)^2 - q^4}}{2|c_1|nq^2}. \tag{8}$$

If we choose ζ_0 to be real and positive, we have $\langle F_x\rangle = \langle F_\perp\rangle\cos\phi$ and $\langle F_y\rangle = \langle F_\perp\rangle\sin\phi$, where $\phi \equiv \chi_1 = -\chi_{-1}$. The longitudinal magnetization, which is parallel to the external magnetic field, is given by

$$\langle F_z\rangle = N_0\frac{p(p^2 + 2|c_1|nq - q^2)}{2|c_1|nq^2}. \tag{9}$$

The total magnetization is therefore given by

$$|\langle \boldsymbol{F}\rangle| \equiv \sqrt{\langle F_\perp\rangle^2 + \langle F_z\rangle^2} = N_0\frac{\sqrt{4c_1^2n^2q^2 - (p^2 - q^2)^2}}{2|c_1|nq}. \tag{10}$$

The magnetization thus tilts against the applied magnetic field with the polar angle

$$\vartheta = \arctan\left(\frac{\sqrt{q^2 - p^2}\sqrt{p^2 + 2|c_1|nq + q^2}}{p\sqrt{p^2 + 2|c_1|nq - q^2}}\right). \tag{11}$$

We note that this ground state breaks the axisymmetry around the z axis despite the fact that the Hamiltonian including the external magnetic field is axisymmetric. Thus the ground state features spontaneous breaking of axisymmetry or spontaneous breaking of the SO(2) symmetry. Such an axisymmetry breaking is due to the competition between the linear and quadratic Zeeman effects and the ferromagnetic interaction. The quadratic Zeeman effect decreases the z component of the spin vector. However, a decrease in the length of the spin vector costs the ferromagnetic interaction energy. To reconcile the quadratic Zeeman effect with the ferromagnetic interaction, the spin vector tilts against the z axis. In fact, ϑ in Eq. (11) is a monotonically decreasing function of p and a monotonically increasing function of q, and the length of the spin vector (10) attains the maximum value of N_0 for $|c_1|n \to \infty$.

III. BOGOLIUBOV EXCITATIONS AND GOLDSTONE MODES

According to the Goldstone theorem [22], there exists a gapless excitation mode when a continuous symmetry is spontaneously broken. In the preceding section, we have shown that in the broken-axisymmetry phase the relevant continuous symmetry is the SO(2) axisymmetry. Since in the MFT the global phase of the wave function is assumed to be arbitrarily chosen, the U(1) symmetry is also broken. Thus the two continuous symmetries are simultaneously broken in this phase. In this section, we examine the corresponding Goldstone modes using the Bogoliubov theory.

A. Number-conserving Bogoliubov theory

We employ the number-conserving Bogoliubov theory [23] for a BEC with spin degrees of freedom [17]. The advantage of the number-conserving formalism is that we do not need to introduce the chemical potential as a Lagrange multiplier in order to adjust the particle number to a prescribed value. In this formulation, we replace $\hat{a}_{\mathbf{0},m}$ with $\zeta_m(N - \Sigma_{\mathbf{k}\neq\mathbf{0},m}\hat{a}^\dagger_{\mathbf{k},m}\hat{a}_{\mathbf{k},m})^{1/2}$ in Eqs. (3) and (4) and keep terms up to those of the second order in $\hat{a}_{\mathbf{k}\neq\mathbf{0},m}$ and $\hat{a}^\dagger_{\mathbf{k}\neq\mathbf{0},m}$. We then obtain an effective Bogoliubov Hamiltonian as [17]

$$\hat{\mathcal{H}}_{\text{eff}} = \sum_{\mathbf{k}\neq\mathbf{0}} \sum_{m=-1}^{1} (\epsilon_{\mathbf{k}} - pm + qm^2 + p\langle f_z\rangle - q\langle f_z^2\rangle - c_1 n + c_1 n|\zeta_0^2 - 2\zeta_1\zeta_{-1}|^2)\hat{a}_{\mathbf{k},m}^\dagger \hat{a}_{\mathbf{k},m} + c_1 n\langle \mathbf{f}\rangle \cdot \sum_{\mathbf{k}\neq\mathbf{0}} \sum_{m,n} \mathbf{f}_{m,n} \hat{a}_{\mathbf{k},m}^\dagger \hat{a}_{\mathbf{k},n} + \frac{c_0 n}{2} \sum_{\mathbf{k}\neq\mathbf{0}} (2\hat{\mathcal{D}}_{\mathbf{k}}^\dagger \hat{\mathcal{D}}_{\mathbf{k}} + \hat{\mathcal{D}}_{\mathbf{k}} \hat{\mathcal{D}}_{-\mathbf{k}} + \hat{\mathcal{D}}_{\mathbf{k}}^\dagger \hat{\mathcal{D}}_{-\mathbf{k}}^\dagger) + \frac{c_1 n}{2} \sum_{\mathbf{k}\neq\mathbf{0}} (2\hat{\boldsymbol{\mathcal{F}}}_{\mathbf{k}}^\dagger \cdot \hat{\boldsymbol{\mathcal{F}}}_{\mathbf{k}} + \hat{\boldsymbol{\mathcal{F}}}_{\mathbf{k}} \cdot \hat{\boldsymbol{\mathcal{F}}}_{-\mathbf{k}} + \hat{\boldsymbol{\mathcal{F}}}_{\mathbf{k}}^\dagger \cdot \hat{\boldsymbol{\mathcal{F}}}_{-\mathbf{k}}^\dagger) + E_0, \tag{12}$$

where $\hat{\mathcal{D}}_{\mathbf{k}} \equiv \Sigma_m \zeta_m^* \hat{a}_{\mathbf{k},m}$, $\hat{\boldsymbol{\mathcal{F}}}_{\mathbf{k}} \equiv \Sigma_{m,n} \mathbf{f}_{m,n} \zeta_m^* \hat{a}_{\mathbf{k},n}$, and E_0 represents a constant term.

In general, for spin-f atoms, we can express quasiparticle operators $\hat{b}_{\mathbf{k},\sigma}$'s as linear combinations of the annihilation and creation operators of the original particles:

$$\hat{\mathbf{B}}_{\mathbf{k}} = U(k)\hat{\mathbf{A}}_{\mathbf{k}} + V(k)\hat{\mathbf{A}}_{-\mathbf{k}}^*. \tag{13}$$

Here $U(k)$ and $V(k)$ are $(2f+1)\times(2f+1)$ real matrices and the bold letters represent sets of operators

$$\hat{\mathbf{B}}_{\mathbf{k}} = {}^T(\hat{b}_{\mathbf{k},\sigma_1}, \hat{b}_{\mathbf{k},\sigma_2}, \ldots, \hat{b}_{\mathbf{k},\sigma_{2f+1}}),$$

$$\hat{\mathbf{A}}_{\mathbf{k}} = {}^T(\hat{a}_{\mathbf{k},f}, \hat{a}_{\mathbf{k},f-1}, \ldots, \hat{a}_{\mathbf{k},-f}),$$

$$\hat{\mathbf{A}}_{\mathbf{k}}^* = {}^T(\hat{a}_{\mathbf{k},f}^\dagger, \hat{a}_{\mathbf{k},f-1}^\dagger, \ldots, \hat{a}_{\mathbf{k},-f}^\dagger),$$

where σ_j is the label for each Bogoliubov mode. The quasiparticle operators (13) should satisfy the Bose commutation relations,

$$[\hat{b}_{\mathbf{k},\sigma}, \hat{b}_{\mathbf{k}',\sigma'}] = 0, \quad [\hat{b}_{\mathbf{k},\sigma}, \hat{b}_{\mathbf{k}',\sigma'}^\dagger] = \delta_{\mathbf{k},\mathbf{k}'}\delta_{\sigma,\sigma'}, \tag{14}$$

which lead to

$$\sum_i [U_{\sigma,i}(k)^T U_{i,\sigma'}(k) - V_{\sigma,i}(k)^T V_{i,\sigma'}(k)] = \delta_{\sigma,\sigma'}, \tag{15}$$

$$\sum_i [U_{\sigma,i}(k)^T V_{i,\sigma'}(k) - V_{\sigma,i}(k)^T U_{i,\sigma'}(k)] = 0. \tag{16}$$

We can rewrite Eqs. (15) and (16) in a matrix form,

$${}^T(U+V)(U-V) = \mathrm{I}. \tag{17}$$

Thus U and V are not independent of each other. For later convenience, we rewrite $\hat{\mathbf{B}}_{\mathbf{k}}$ as

$$\hat{\mathbf{B}}_{\mathbf{k}} = \frac{1}{2}[(U+V)(\hat{\mathbf{A}}_{\mathbf{k}} + \hat{\mathbf{A}}_{-\mathbf{k}}^*) + (U-V)(\hat{\mathbf{A}}_{\mathbf{k}} - \hat{\mathbf{A}}_{-\mathbf{k}}^*)]. \tag{18}$$

We seek the excitation spectrum E_σ and the corresponding Bogoliubov operators $\hat{b}_{\mathbf{k},\sigma}$ such that the quasiparticles behave independently, i.e.,

$$\hat{\mathcal{H}}_{\text{eff}} = \sum_{\mathbf{k}\neq\mathbf{0}} \sum_{\sigma=\{\sigma_1,\sigma_2,\ldots,\sigma_{2f+1}\}} E_\sigma \hat{b}_{\mathbf{k},\sigma}^\dagger \hat{b}_{\mathbf{k},\sigma} + E_{\text{vac}}, \tag{19}$$

where $\hat{\boldsymbol{\mathcal{H}}}_{\text{eff}}$ is given in Eq. (12) and E_{vac} is the energy of the vacuum state for the quasiparticles. From Eq. (12), the Heisenberg equation of motion takes the form

$$i\hbar \frac{d}{dt}\hat{\mathbf{A}}_{\mathbf{k}} = M(k)\hat{\mathbf{A}}_{\mathbf{k}} + N(k)\hat{\mathbf{A}}_{-\mathbf{k}}^*, \tag{20}$$

where $M(k)$ and $N(k)$ are real and symmetric $(2f+1)\times(2f+1)$ matrices. Using the quasiparticle Hamiltonian (19) and the commutation relations (14), we obtain

$$i\hbar \frac{d}{dt}\hat{\mathbf{B}}_{\mathbf{k}} = E(k)\hat{\mathbf{B}}_{\mathbf{k}}, \tag{21}$$

where $E(k)$ is the diagonal $(2f+1)\times(2f+1)$ matrix, whose diagonal elements correspond to the energies of the elementary excitations $E_{\mathbf{k},\sigma_j}$. Then by substituting Eq. (20) into Eq. (21) and using Eq. (17), we obtain

$$(M+N)(M-N)^T(U+V) = {}^T(U+V)E^2. \tag{22}$$

Since E^2 is also a diagonal matrix, the Bogoliubov excitation spectrum can be found as the eigenvalues of the matrix

$$G \equiv (M+N)(M-N). \tag{23}$$

We note that G, which is the product of two Hermitian matrices, is not, in general, Hermitian. The present approach has the advantage that we can reduce the dimension of the eigenvalue equation from $2(2f+1)$ to $(2f+1)$ and therefore the diagonalization is simplified. That is, instead of the diagonalization of the $2(2f+1)\times 2(2f+1)$ matrix as

$$\begin{pmatrix} M & N \\ -N & -M \end{pmatrix} \to \begin{pmatrix} E & 0 \\ 0 & -E \end{pmatrix}, \tag{24}$$

the $(2f+1)\times(2f+1)$ matrix G is to be diagonalized.

B. Low-lying modes in the broken-axisymmety phase for $\mathbf{k}\to\mathbf{0}$

Without loss of generality, we can assume ζ_m to be real and positive. The excitation spectra in the ferromagnetic and polar phases can be derived analytically as shown in Appendix B. The analytic solutions can also be obtained for the broken-axisymmetry phase for general k. However, since they are very complicated, we derive here the excitation spectrum for small k.

The effective Hamiltonian (12) gives the coefficient matrices M and N of the Heisenberg equation of motion (20). Using the explicit form of ζ_m in Eq. (7), the matrix G can be written in the form

$$G = G_0 + 2(g_2 n G_1 - c_1 n G_1')\epsilon_{\mathbf{k}} + I\epsilon_{\mathbf{k}}^2, \tag{25}$$

where I is the unit matrix and

$$G_0 = \begin{pmatrix} \Theta_1\zeta_{-1}\zeta_0 & \Theta_1\zeta_1\zeta_{-1} & \Theta_1\zeta_1\zeta_0 \\ \Theta_0\zeta_{-1}\zeta_0 & \Theta_0\zeta_1\zeta_{-1} & \Theta_0\zeta_1\zeta_0 \\ \Theta_{-1}\zeta_{-1}\zeta_0 & \Theta_{-1}\zeta_1\zeta_{-1} & \Theta_{-1}\zeta_1\zeta_0 \end{pmatrix}, \tag{26}$$

$$G_1 = \begin{pmatrix} \zeta_1^2 & \zeta_1\zeta_0 & \zeta_1\zeta_{-1} \\ \zeta_1\zeta_0 & \zeta_0^2 & \zeta_{-1}\zeta_0 \\ \zeta_1\zeta_{-1} & \zeta_{-1}\zeta_0 & \zeta_{-1}^2 \end{pmatrix}, \tag{27}$$

$$G_1' = \begin{pmatrix} \zeta_0^2\zeta_{-1}/\zeta_1 & -2\zeta_{-1}\zeta_0 & -2\zeta_1\zeta_{-1} \\ -2\zeta_{-1}\zeta_0 & \zeta_0^2 + 2\zeta_1\zeta_{-1} & -2\zeta_{-1}\zeta_0 \\ -2\zeta_1\zeta_{-1} & -2\zeta_{-1}\zeta_0 & \zeta_0^2\zeta_1/\zeta_{-1} \end{pmatrix}, \tag{28}$$

with

$$\Theta_m = (3m^2 - 2)|c_1|n[p^2 + 2|c_1|nq + (-1)^m q^2 - 2mpq]\zeta_0/(q\zeta_m). \tag{29}$$

We first consider the limit of $\mathbf{k} \to \mathbf{0}$. The three eigenvalues for $G = G_0$ can be obtained easily: One is

$$E_{\text{gap}}^2 = (3p^2 - 2c_1nq - q^2)(p^2 - 2c_1nq + q^2)/q^2 \tag{30}$$

and the other two are zero. Thus the system has two gapless excitation modes, which, as we will show later, originate from the U(1) and SO(2) symmetry breakings. We label the gapful mode as α and the two gapless modes as β and γ.

The eigenvectors of G_0 are given by each row of the following matrix:

$$U + V = \begin{pmatrix} \lambda\Theta_1 & \lambda\Theta_0 & \lambda\Theta_{-1} \\ (\mu_p + \mu_m)\zeta_1 & \mu_p\zeta_0 & (\mu_p - \mu_m)\zeta_{-1} \\ (\nu_p + \nu_m)\zeta_1 & \nu_p\zeta_0 & (\nu_p - \nu_m)\zeta_{-1} \end{pmatrix}, \tag{31}$$

where λ, μ_p, μ_m, ν_p, and ν_m are arbitrary parameters. Note that the second and third rows can be expressed as the linear combinations of two vectors $(\zeta_1, \zeta_0, \zeta_{-1})$ and $(\zeta_1, 0, -\zeta_{-1})$, both of which are eigenvectors with zero eigenvalues. It follows from Eq. (17) that the matrix $U - V$ is given as the transposed inverse matrix of Eq. (31):

$$U - V = \frac{1}{A}\begin{pmatrix} \dfrac{\zeta_{-1}\zeta_0}{\lambda} & 2\dfrac{\zeta_1\zeta_{-1}}{\lambda} & \dfrac{\zeta_1\zeta_0}{\lambda} \\ \dfrac{-\zeta_{-1}\Theta_0(\nu_p - \nu_m) + \zeta_0\Theta_{-1}\nu_p}{J} & \dfrac{\zeta_{-1}\Theta_1(\nu_p - \nu_m) - \zeta_1\Theta_{-1}(\nu_p + \nu_m)}{J} & \dfrac{\zeta_1\Theta_0(\nu_p + \nu_m) - \zeta_0\Theta_1\nu_p}{J} \\ \dfrac{\zeta_{-1}\Theta_0(\mu_p - \mu_m) - \zeta_0\Theta_{-1}\mu_p}{J} & \dfrac{-\zeta_{-1}\Theta_1(\mu_p - \mu_m) + \zeta_1\Theta_{-1}(\mu_p + \mu_m)}{J} & \dfrac{-\zeta_1\Theta_0(\mu_p + \mu_m) + \zeta_0\Theta_1\mu_p}{J} \end{pmatrix}, \tag{32}$$

where $A \equiv 2\zeta_1\zeta_{-1}\Theta_0 - \zeta_0\zeta_{-1}\Theta_1 - \zeta_0\zeta_1\Theta_{-1}$ and $J \equiv \mu_p\nu_m - \mu_m\nu_p$.

C. Low-lying modes in the broken-axisymmetry phase for small k

In the limit of small $\mathbf{k}$, the five parameters λ, μ_p, μ_m, ν_p, and ν_m can be determined by substituting Eqs. (31) and (32) into the definitions of the Bogoliubov operators (18) and by comparing the quasiparticle Hamiltonian (19) with the effective Hamiltonian (12). However, we cannot perform this procedure by using the expressions of the eigenvectors for $\mathbf{k} = \mathbf{0}$ because the two Goldstone modes diverge in the limit of $\mathbf{k} \to \mathbf{0}$. Thus it is necessary to find the $\epsilon_{\mathbf{k}}$ dependence of the eigenenergies in order to find the properties of the low-lying excitations. From Eqs. (26)–(28), we obtain the eigenenergies up to the order of $\epsilon_{\mathbf{k}}$ as

$$E_\alpha^2 = E_{\text{gap}}^2 + 4\left(\frac{p^2 - c_1nq}{q}\right)\epsilon_{\mathbf{k}} + O(\epsilon_{\mathbf{k}}^2),$$

$$E_\beta^2 = \Lambda_+\epsilon_{\mathbf{k}} + O(\epsilon_{\mathbf{k}}^2),$$

$$E_\gamma^2 = \Lambda_-\epsilon_{\mathbf{k}} + O(\epsilon_{\mathbf{k}}^2), \tag{33}$$

where

$$\Lambda_\pm = g_2n + \frac{\eta}{2} \pm \frac{1}{2}\sqrt{(2g_2n - \eta)^2 + \frac{8g_2n(q - \eta)\eta^2}{c_1n(3\eta - 2q + 2c_1n)}}$$

with $\eta = (q^2 - p^2)/q$. In Fig. 3, we compare the $\epsilon_{\mathbf{k}}$ dependences of the approximate eigenenergies (33) (dashed curves) with those of the numerically obtained exact energies (solid curves).

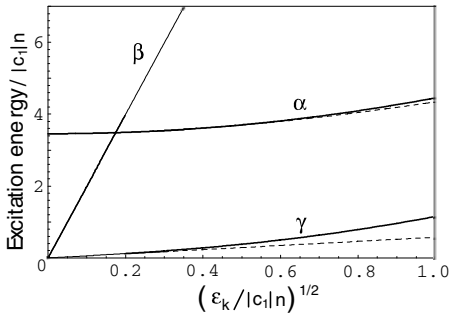

FIG. 3. Excitation spectrum in the broken-axisymmetry phase. The solid curves represent the numerically obtained exact solutions and the dashed curves are approximate solutions in Eq. (33). The linear and quadratic Zeeman coefficients are chosen to be $p/|c_1|n = 9/10$ and $q/|c_1|n = 11/10$. The modes β and γ are the gapless modes associated with the simultaneous breakings of U(1) and SO(2) symmetries. The exact and approximate solutions for the β mode cannot be resolved in this figure.

It is important to note that the two gapless excitations E_β and E_γ in Eq. (33) share the same leading-order term $\epsilon_{\mathbf{k}}^{1/2}$. Since the effective Hamiltonian $\hat{\mathcal{H}}_{\text{eff}}$ in Eq. (12) contains only the terms that are proportional to $\epsilon_{\mathbf{k}}$, this $\epsilon_{\mathbf{k}}^{1/2}$ dependence must be canceled by the factors in the operators $\hat{b}_{\mathbf{k},\sigma}$ so that Eq. (19) reproduces Eq. (12). Therefore, we find that the normalization factors μ_p, μ_m, ν_p, and ν_m in Eq. (31), which determines $\hat{b}_{\mathbf{k},\sigma}$ through Eq. (13), must be proportional to either $\epsilon_{\mathbf{k}}^{-1/4}$ or $\epsilon_{\mathbf{k}}^{1/4}$. From numerical analysis, we find that they all have an $\epsilon_{\mathbf{k}}^{-1/4}$ dependence as do the cases of gapless excitations in the other phases (see Appendix B). It follows then from Eqs. (31) and (32) that $(U+V)_{\sigma,m} \sim O(\epsilon_{\mathbf{k}}^{-1/4})$ and $(U-V)_{\sigma,m} \sim O(\epsilon_{\mathbf{k}}^{1/4})$, and

$$(U+V)_{\sigma,m} \gg (U-V)_{\sigma,m} \quad (\sigma=\beta \text{ or } \gamma) \tag{34}$$

for $\epsilon_{\mathbf{k}} \to 0$. Therefore, we can neglect the second term in the square bracket in Eq. (18), obtaining

$$\hat{b}_{\mathbf{k},\sigma} \simeq \sum_m (U+V)_{\sigma,m}(\hat{a}_{\mathbf{k},m} + \hat{a}^\dagger_{-\mathbf{k},m}) \tag{35}$$

for $\sigma=\beta$ and γ. The corresponding Bogoliubov operators are then written as

$$\hat{b}_{\mathbf{k},\beta} \simeq \mu_p \sum_m \zeta_m(\hat{a}_{\mathbf{k},m} + \hat{a}^\dagger_{-\mathbf{k},m}) + \mu_m \sum_m m\zeta_m(\hat{a}_{\mathbf{k},m} + \hat{a}^\dagger_{-\mathbf{k},m}),$$

$$\hat{b}_{\mathbf{k},\gamma} \simeq \nu_p \sum_m \zeta_m(\hat{a}_{\mathbf{k},m} + \hat{a}^\dagger_{-\mathbf{k},m}) + \nu_m \sum_m m\zeta_m(\hat{a}_{\mathbf{k},m} + \hat{a}^\dagger_{-\mathbf{k},m}). \tag{36}$$

Equation (36) indicates that the quasiparticle operators for the two gapless modes are constituted from the number fluctuation operator

$$\delta\hat{N} = \sqrt{N_0}\left[\sum_m \zeta_m(\hat{a}_{\mathbf{k},m} + \hat{a}^\dagger_{-\mathbf{k},m})\right] \tag{37}$$

and the spin fluctuation operator

$$\delta\hat{F}_z = \sqrt{N_0}\left[\sum_m m\zeta_m(\hat{a}_{\mathbf{k},m} + \hat{a}^\dagger_{-\mathbf{k},m})\right]. \tag{38}$$

We recall that the operator $\hat{N}$ is the generator of the global phase rotation and the operator $\hat{F}_z$ is that of the spin rotation around the z axis. The creations of the gapless quasiparticles therefore lead to translation in the global phase of the order parameter and rotation of the magnetization around the z axis. The modes β and γ are thus the Goldstone modes that restore the U(1) and SO(2) symmetries. Since $\delta\hat{N}$ and $\delta\hat{F}_z$ can be regarded as the phonon and magnon operators, respectively, phonons and magnons are coupled in the quasiparticles described by Eq. (36). This is in contrast to the cases of the ferromagnetic and polar phases, in which phonons and magnons are decoupled (see Appendix B). The numerically obtained coefficients μ_p, μ_m, ν_p, and ν_m are shown in Fig. 4 as functions of $q/|c_1|n$. We see that $\hat{b}_{\mathbf{k},\beta}$ is predominantly the density fluctuation operator, while $\hat{b}_{\mathbf{k},\gamma}$ is the linear combination of the number and spin fluctuation operators with roughly equal weights for small $q/|c_1|n$. In other words, the β mode is a phonon-dominant mode and the γ mode is a phonon-magnon coupled mode. The β mode crosses over to a phonon mode across the two neighboring phase boundaries, while the γ mode crosses over to a magnon mode.

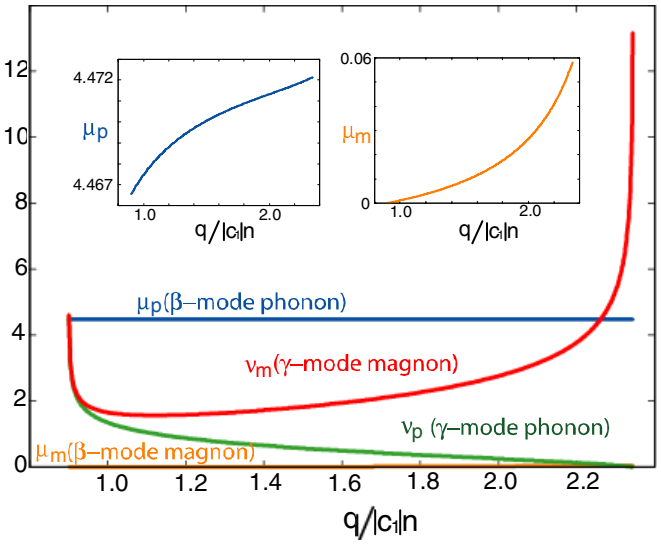

FIG. 4. (Color online) Coefficients in the phonon-magnon modes [μ_p, μ_m, ν_p, and ν_m in Eq. (36)] as functions of the normalized quadratic Zeeman energy $q/|c_1|n$. The linear Zeeman energy is chosen to be $p/|c_1|n=9/10$. The vertical axis is scaled by $(\epsilon_{\mathbf{k}}/|c_1|n)^{1/4}/\sqrt{N_0}$. The values of the scattering lengths obtained by Kempen *et al.* [21] are used: $a_0=101.8$ a.u. and $a_2=100.4$ a.u. The insets show the enlarged curves for μ_p and μ_m.

D. Coherent excitations

We investigate the dynamics of the system when the quasiparticles are coherently excited. The excited state is assumed to be a coherent state

$$|\beta_{k,\sigma}\rangle \equiv e^{\beta_{k,\sigma}\hat{b}^\dagger_{\mathbf{k},\sigma} - \beta^*_{k,\sigma}\hat{b}_{\mathbf{k},\sigma}}|0\rangle_B, \tag{39}$$

where $|0\rangle_B$ is the vacuum of the Bogoliubov quasiparticles. The change in the expectation value of an observable $\hat{Q}$ due to the excitation of quasiparticles is given by

$$\langle\delta\hat{Q}_{\mathbf{k},\sigma}(t)\rangle = \langle\beta_{k,\sigma}|\hat{Q}_H(t)|\beta_{k,\sigma}\rangle - {}_B\langle 0|\hat{Q}_H(t)|0\rangle_B, \tag{40}$$

where the subscript H denotes the Heisenberg representation. Since $\hat{\mathbf{A}}_{\mathbf{k}} = {}^TU(k)\hat{\mathbf{B}}_{\mathbf{k}} - {}^TV(k)\hat{\mathbf{B}}^*_{-k}$ using the inverse relation of Eq. (13), we obtain

$$\langle\delta\hat{\Psi}_m(t)\rangle_{\mathbf{k},\sigma} = \frac{|\beta_{k,\sigma}|}{\sqrt{\Omega}}[(U-V)_{\sigma,m}\cos(\mathbf{k}\cdot\mathbf{r} - \omega_\sigma t + \phi_{k,\sigma}) + i(U+V)_{\sigma,m}\sin(\mathbf{k}\cdot\mathbf{r} - \omega_\sigma t + \phi_{k,\sigma})], \tag{41}$$

where $\phi_{k,\sigma}=\arg(\beta_{k,\sigma})$ and $\omega_\sigma = E_{\mathbf{k},\sigma}/\hbar$. Since the ratio of the real part to the imaginary part is estimated from Eq. (34) to be $(\bar{\epsilon}_{\mathbf{k}})^{1/2} \ll 1$, the real part is negligible for the two gapless modes, $\sigma=\beta$ and γ, in the long-wavelength limit. Therefore, $\langle\delta\hat{\Psi}_m(t)\rangle_{\mathbf{k},\sigma}$ is almost purely imaginary, indicating that the

change occurs mostly in the phase of the order parameter ζ_m. Thus the excitations of the β and γ modes lead to a global phase rotation and a spin rotation around the z axis.

To study how the quasiparticle excitation rotates the spin, we calculate $\langle \delta\hat{\mathbf{F}}(t)\rangle_{\mathbf{k},\sigma}$. Keeping terms up to those of the first order in $\beta_{k,\sigma}$, we obtain

$$\langle \delta\hat{F}_\xi(t)\rangle_{\mathbf{k},\sigma} = \frac{\sqrt{n_0}}{\sqrt{\Omega}}\sum_{m,n}\zeta_m(f_\xi)_{m,n} \times[(U \mp V)_{\sigma,n}e^{i(\mathbf{k}\cdot\mathbf{r}-\omega_\sigma t)}\beta_{k,\sigma} \pm \text{H.c.}], \quad (42)$$

where f_ξ ($\xi=x,y,z$) are the spin-1 matrices defined in Eq. (A13), and the upper signs refer to $\xi=x$ and z and the lower signs to $\xi=y$. Hence, Eq. (34) leads to $\langle \delta\hat{F}_y\rangle_{\mathbf{k},\sigma} \gg \langle \delta\hat{F}_x\rangle_{\mathbf{k},\sigma}$ and $\langle \delta\hat{F}_y\rangle_{\mathbf{k},\sigma} \gg \langle \delta\hat{F}_z\rangle_{\mathbf{k},\sigma}$. This is because $\langle \hat{F}_x\rangle \neq 0$, $\langle \hat{F}_z\rangle \neq 0$, and $\langle \hat{F}_y\rangle = 0$ from the assumption of real and positive ζ_m, and the infinitesimal spin rotation around the z axis predominantly changes $\langle \hat{F}_y\rangle$.

We have shown that the excitations of the Goldstone modes β and γ lead to U(1) and SO(2) transformations. Oscillations of the order-parameter phases and those of the azimuthal angle of the spin vector are shown in Fig. 5. Figure 5(a) shows that excitations of the β mode change the phases of $\langle \hat{\psi}_1\rangle$, $\langle \hat{\psi}_0\rangle$, and $\langle \hat{\psi}_{-1}\rangle$ in the same manner. This is because, as shown in Fig. 4, the dominant contribution to the β mode is made by phonons which are insensitive to individual spin components. On the other hand, the γ-mode excitation describes not only fluctuations of the overall phase but also those of the spin vector around the z axis. Since the rotation around the z axis is $e^{i\varphi\hat{F}_z}|m\rangle = e^{i\varphi m}|m\rangle$, χ_1 and χ_{-1} are out of phase with respect to χ_0.

The gapful mode (α mode) can be interpreted as playing the role of changing the magnitude of magnetization. As shown in Fig. 6, the fluctuation of F_x is dominant when the α mode is excited. The z component F_z cannot vary due to the spin conservation, and hence the spin fluctuation is restricted in the x-y plane, as illustrated in the inset of Fig. 6.

IV. DISCUSSION

We have shown that the ground state in the shaded region of Fig. 1 is the broken-axisymmetry phase which features transverse magnetization. Here, we discuss possible experimental consequences of the axisymmetry breaking and the transverse magnetization.

We have considered so far the case in which the axisymmetry is broken uniformly over the entire system. However, starting from a nonmagnetic state, e.g., the $m=0$ state, the system cannot develop into the uniformly broken-axisymmetry state, since the total spin angular-momentum component parallel to the magnetic field must be conserved, and for small q the magnitude of the transverse component of the total spin is nearly entirely conserved. For such an initial state, directions of the axisymmetry breaking should vary randomly in space while conserving the projected total spin angular momentum, and various spin textures are formed depending on the trap geometry [24,25]. For example, in an elongated cigar-shaped trap, a staggered domain structure or a helical structure is expected to develop spontaneously [24]. In a pancake-shaped trap, on the other hand, a concentric domain structure will be formed [24].

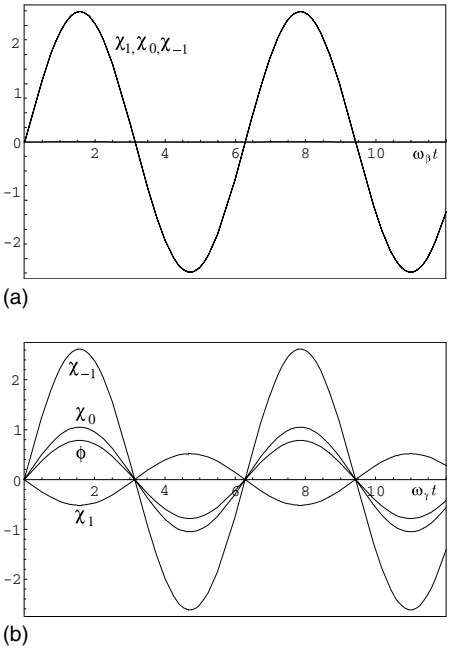

FIG. 5. Oscillations of the order-parameter phases ($\chi_m \equiv \tan^{-1}[\mathrm{Im}\langle\hat{\psi}_m\rangle/\mathrm{Re}\langle\hat{\psi}_m\rangle]$) and the azimuthal angle of magnetization around the z axis ($\phi \equiv \tan^{-1}[\langle\hat{F}_y\rangle/\langle\hat{F}_x\rangle]$) caused by the excitation of the Bogoliubov quasiparticles in the long-wavelength limit. The ordinates are marked in arbitrary units, and the Zeeman energies are taken to be $p/|c_1|n=9/10$ and $q/|c_1|n=11/10$. (a) Phonon-dominant mode (β mode). Since rotation of the magnetization occurs much slower than rotations of the order parameter phases, we cannot see the latter (ϕ) in this figure. (b) Phonon-magnon coupled mode (γ mode).

Another interesting possibility is a topological spin texture, in which the orientation of transverse magnetization has a 2π winding about a central defect [25]. The direction of the winding can be clockwise or counterclockwise which is chosen spontaneously. Therefore, this state breaks the chiral symmetry as well as the axisymmetry.

Recently, spontaneous magnetization of a ^{87}Rb BEC has been observed by the Berkeley group [19] under conditions

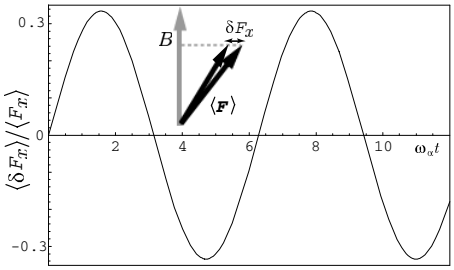

FIG. 6. Oscillation of transverse magnetization $\langle F_x\rangle$ due to coherent excitations of the gapful mode (α mode). The inset schematically illustrates a change in the spin vector caused by the excitation of the α mode.

in which the state of the system is changed rapidly by a change in the magnetic field from the $|0\rangle$ region to the shaded region in Fig. 1. The spontaneous transverse magnetization observed in the Berkeley experiment is therefore a manifestation of the symmetry breaking discussed in the present paper. In this experiment, a topological spin texture predicted in Ref. [25] was also detected as a spin vortex. In the Berkeley experiment, the magnetic field is rapidly changed from the polar phase to the broken-axisymmetry phase and the system is significantly disturbed. If the speed of the change is slow, on the other hand, the system will be only weakly disturbed, and low-energy gapless excitations (the β and γ modes) predicted in this paper should be observed.

V. CONCLUSIONS

We have studied a spin-1 ferromagnetic BEC by taking the quadratic Zeeman effect into account. The mean field theory predicts that BECs with ferromagnetic interactions have the broken-axisymmetry phase, in which magnetization tilts against the direction of an external magnetic field. Here, the SO(2) symmetry is broken, in addition to the U(1) global phase symmetry. Applying the Bogoliubov theory for a BEC with spin degrees of freedom, we have found one gapful mode and two gapless Goldstone modes for this phase. We have analytically shown that two gapless modes are the coupled phonon-magnon modes that restore the U(1) and SO(2) symmetries simultaneously. Numerical analysis has shown that one Goldstone mode is the phonon-dominant mode and the other is the phonon-magnon coupled mode with roughly equal weights. The gapful mode changes the magnitude of the spin by fluctuating the spin in the direction perpendicular to the magnetic field (see the inset of Fig. 6).

When more than one continuous symmetry is spontaneously broken, multiple gapless modes emerge which are coupled to generate the same number of Goldstone modes as that of the broken symmetries. When two gapless modes are coupled, they usually anticross and develop a gapful mode such as optical phonons and plasmons. This rule does not apply to the present case because both of the gapless modes originate from broken continuous symmetries. Similar phenomena may be expected in spin-2 BECs [12] and higher spin BECs, which merit further investigation.

ACKNOWLEDGMENTS

We thank T. Mori for his participation in an early stage of this work. This work was supported by Grants-in-Aid for Scientific Research (Grant Nos. 17071005 and 17740263) and by the 21st Century COE programs on "Nanometer-Scale Quantum Physics" and "Coherent Optical Science" from the Ministry of Education, Culture, Sports, Science and Technology of Japan. M.U. acknowledges support from a CREST program of the JST.

APPENDIX A: DERIVATION OF THE PHASE DIAGRAM FOR $c_1<0$

In this Appendix, we derive the analytic expression for the spinor components in Eq. (7) in the broken-axisymmetry phase and reproduce the phase diagram for $c_1<0$ in Fig. 1.

The average energy per atom is given from Eq. (5) by

$$e \equiv \frac{|c_1|n}{2}|2\zeta_1\zeta_{-1}-\zeta_0^2|^2+\sum_{m=-1}^{1}(-pm+qm^2)|\zeta_m|^2, \quad \text{(A1)}$$

where we omit the spin-independent energy $c_0n/2$. The first term on the right-hand side of Eq. (A1) can be rewritten as

$$\frac{|c_1|n}{2}|2\zeta_1\zeta_{-1}-\zeta_0^2|^2=\frac{|c_1|n}{2}|2|\zeta_1\zeta_{-1}|-|\zeta_0|^2e^{i(2\chi_0-\chi_1-\chi_{-1})}|^2, \quad \text{(A2)}$$

where $\zeta_m=|\zeta_m|e^{i\chi_m}$. Hence the phase depends on energy only through $2\chi_0-\chi_1-\chi_{-1}$, and the energy is minimized for $2\chi_0-\chi_1-\chi_{-1}=0$. Without loss of generality, we assume that ζ_m's are real and non-negative.

We minimize

$$K \equiv e-\mu(\zeta_1^2+\zeta_0^2+\zeta_{-1}^2), \quad \text{(A3)}$$

where μ is a Lagrange multiplier which is introduced to ensure the normalization condition $\zeta_1^2+\zeta_0^2+\zeta_{-1}^2=1$. Stationary conditions can be obtained through differentiation of K with respect to ζ_m's as

$$\frac{\partial K}{\partial \zeta_{\pm 1}}=2|c_1|n(2\zeta_1\zeta_{-1}-\zeta_0^2)\zeta_{\mp 1}+2(q\mp p-\mu)\zeta_{\pm 1}=0, \quad \text{(A4)}$$

$$\frac{\partial K}{\partial \zeta_0}=-2|c_1|n(2\zeta_1\zeta_{-1}-\zeta_0^2)\zeta_0-2\mu\zeta_0=0. \quad \text{(A5)}$$

It follows from Eq. (A5) that either $\zeta_0=0$ or

$$\mu=-|c_1|n(2\zeta_1\zeta_{-1}-\zeta_0^2) \quad \text{(A6)}$$

has to be satisfied. When $\zeta_0=0$, we find that K is minimized with

$$\zeta_1=1, \quad \zeta_{-1}=0 \text{ for } p>0 \quad (e=q-p), \quad \text{(A7)}$$

$$\zeta_1=0, \quad \zeta_{-1}=1 \text{ for } p<0 \quad (e=q+p). \quad \text{(A8)}$$

When $\zeta_0\neq 0$, Eq. (A4) becomes

$$(q\mp p-\mu)\zeta_{\pm 1}=\mu\zeta_{\mp 1}. \quad \text{(A9)}$$

We can easily see that the polar state

$$\zeta_0=1, \quad \zeta_1=\zeta_{-1}=0 \quad (e=1) \quad \text{(A10)}$$

satisfies Eq. (A9). Solving Eqs. (A6) and (A9), and the normalization condition for ζ_m, we obtain the solution for the broken-axisymmetry phase in Eq. (7). This solution is valid for

$$q^2-p^2\geq 0 \quad \text{and } 2|c_1|nq-q^2+p^2\geq 0. \quad \text{(A11)}$$

The energy of the broken-axisymmetry state is calculated to be

$$e_{\rm br} = \frac{1}{4(|c_1|nq)^2}(q^2-p^2)(p^2-4|c_1|nq-q^2). \quad \text{(A12)}$$

We can show that $e_{\rm br} \leqslant 1$ and $e_{\rm br} \leqslant q \pm p$ are always satisfied in the region specified by Eq. (A11), and thus we obtain the phase diagram in Fig. 1.

The three components of the spin-1 matrices are given by

$$f_x = \frac{1}{\sqrt{2}}\begin{pmatrix} 0 & 1 & 0 \\ 1 & 0 & 1 \\ 0 & 1 & 0 \end{pmatrix}, \quad f_y = \frac{i}{\sqrt{2}}\begin{pmatrix} 0 & -1 & 0 \\ 1 & 0 & -1 \\ 0 & 1 & 0 \end{pmatrix},$$

$$f_z = \begin{pmatrix} 1 & 0 & 0 \\ 0 & 0 & 0 \\ 0 & 0 & -1 \end{pmatrix}, \quad \text{(A13)}$$

and the corresponding spin components are given by

$$\langle F_x \rangle \equiv N_0 \boldsymbol{\zeta}^\dagger f_x \boldsymbol{\zeta} = \frac{N_0}{\sqrt{2}}[\zeta_0^*(\zeta_1+\zeta_{-1}) + \zeta_0(\zeta_1^*+\zeta_{-1}^*)], \quad \text{(A14)}$$

$$\langle F_y \rangle \equiv N_0 \boldsymbol{\zeta}^\dagger f_y \boldsymbol{\zeta} = i\frac{N_0}{\sqrt{2}}[\zeta_0^*(\zeta_1-\zeta_{-1}) - \zeta_0(\zeta_1^*-\zeta_{-1}^*)], \quad \text{(A15)}$$

$$\langle F_z \rangle \equiv N_0 \boldsymbol{\zeta}^\dagger f_z \boldsymbol{\zeta} = N_0(|\zeta_1|^2 - |\zeta_{-1}|^2). \quad \text{(A16)}$$

Substituting Eq. (7) into Eqs. (A14)–(A16), we obtain Eqs. (8)–(10).

APPENDIX B: EXCITATION SPECTRA IN THE FERROMAGNETIC AND POLAR PHASES

1. Ferromagnetic phase

We first consider the ferromagnetic phase ($|+1\rangle$ in Fig. 1) for $p>0$. In this phase the order parameters are given by $\zeta_1=1$ and $\zeta_0=\zeta_{-1}=0$. The matrices M and N in Eq. (20) are shown to be

$$M = \begin{pmatrix} \epsilon_{\mathbf{k}}+c_0n+c_1n & 0 & 0 \\ 0 & \epsilon_{\mathbf{k}}+p-q & 0 \\ 0 & 0 & \epsilon_{\mathbf{k}}+2p-2c_1n \end{pmatrix}, \quad \text{(B1)}$$

$$N = \begin{pmatrix} c_0n+c_1n & 0 & 0 \\ 0 & 0 & 0 \\ 0 & 0 & 0 \end{pmatrix}, \quad \text{(B2)}$$

and the matrix G in Eq. (23) is given by

$$G = \begin{pmatrix} \epsilon_{\mathbf{k}}(\epsilon_{\mathbf{k}}+2g_2n) & 0 & 0 \\ 0 & (\epsilon_{\mathbf{k}}+p-q)^2 & 0 \\ 0 & 0 & (\epsilon_{\mathbf{k}}-2p-2c_1n)^2 \end{pmatrix}. \quad \text{(B3)}$$

Hence we obtain three excitation energies as

$$E_p = \sqrt{\epsilon_{\mathbf{k}}(\epsilon_{\mathbf{k}}+2g_2n)},$$

$$E_0 = \epsilon_{\mathbf{k}}+p-q,$$

$$E_{-1} = \epsilon_{\mathbf{k}}-2p-2c_1n, \quad \text{(B4)}$$

and the associated quasiparticle operators as

$$\hat{b}_{\mathbf{k},p} = \frac{\sqrt{\epsilon_{\mathbf{k}}+g_2n+E_p}}{\sqrt{2E_p}}\hat{a}_{\mathbf{k},1} + \frac{\sqrt{\epsilon_{\mathbf{k}}+g_2n-E_p}}{\sqrt{2E_p}}\hat{a}^\dagger_{-\mathbf{k},1},$$

$$\hat{b}_{\mathbf{k},0} = \hat{a}_{\mathbf{k},0},$$

$$\hat{b}_{\mathbf{k},-1} = \hat{a}_{\mathbf{k},-1}. \quad \text{(B5)}$$

The corresponding results for $p<0$ can be obtained by changing the linear Zeeman term p to $-p$. For $q=0$, these results reduce to those obtained in the absence of the quadratic Zeeman effect [17]. The excitation spectrum E_p is similar to the one obtained for scalar BECs; it is a phonon mode with the speed of sound given by $c=\sqrt{g_2n/M}$. The other two modes are associated with excitations from the $m=1$ state to the $m=0$ and $m=-1$ states, respectively. In the long-wavelength limit ($k\to 0$), E_0 (E_{-1}) coincides with the single-particle energy difference between the $m=1$ state and the $m=0$ ($m=-1$) state. Hence the phonon mode (E_p) and the magnon modes (E_0, E_{-1}) are decoupled in the ferromagnetic phase.

It can be easily verified that these excitation modes and operators do reproduce the effective Hamiltonian (12) through Eq. (19). For small $\epsilon_{\mathbf{k}}$, E_p in Eq. (B4) is proportional to $\epsilon_{\mathbf{k}}^{1/2}$ and $\hat{b}_{\mathbf{k},p}$ in Eq. (B5) is proportional to $\epsilon_{\mathbf{k}}^{-1/4}$. The singular $\epsilon_{\mathbf{k}}$ dependence in each of E_p and $\hat{b}_{\mathbf{k},p}$ is therefore canceled in the product $E_p\hat{b}^\dagger_{\mathbf{k},p}\hat{b}_{\mathbf{k},p}$, giving the original $\epsilon_{\mathbf{k}}$ dependence in the effective Hamiltonian.

2. Polar phase

In the polar phase ($|0\rangle$ in Fig. 1), the order parameters are $\zeta_0=1$ and $\zeta_1=\zeta_{-1}=0$, and the matrices M and N have the forms

$$M = \begin{pmatrix} \epsilon_{\mathbf{k}}-p+q+c_1n & 0 & \\ 0 & \epsilon_{\mathbf{k}}+c_0n & 0 \\ 0 & 0 & \epsilon_{\mathbf{k}}+p+q+c_1n \end{pmatrix}, \quad \text{(B6)}$$

$$N = \begin{pmatrix} 0 & 0 & c_1n \\ 0 & c_0n & 0 \\ c_1n & 0 & 0 \end{pmatrix}, \quad \text{(B7)}$$

which give

$$G = \begin{pmatrix} (\epsilon_{\mathbf{k}} - p + q + c_1 n)^2 - c_1 n^2 & 0 & 2c_1 np \\ 0 & \epsilon_{\mathbf{k}}(\epsilon_{\mathbf{k}} + 2c_0 n) & 0 \\ -2c_1 np & 0 & (\epsilon_{\mathbf{k}} + p + q + c_1 n)^2 - c_1 n^2 \end{pmatrix}. \tag{B8}$$

Diagonalizing G in Eq. (B8), we obtain the eigenvalues as

$$E_p = \sqrt{\epsilon_{\mathbf{k}}(\epsilon_{\mathbf{k}} + 2c_0 n)},$$

$$E_+ = -p + \xi_{\mathbf{k}},$$

$$E_- = +p + \xi_{\mathbf{k}}, \tag{B9}$$

where $\xi_{\mathbf{k}} = \sqrt{(\epsilon_{\mathbf{k}} + q)(\epsilon_{\mathbf{k}} + q + 2c_1 n)}$. The quasiparticle operators are found to be

$$\hat{b}_{\mathbf{k},p} = \frac{\sqrt{\epsilon_{\mathbf{k}} + c_0 n + E_p}}{\sqrt{2E_p}} \hat{a}_{\mathbf{k},0} + \frac{\sqrt{\epsilon_{\mathbf{k}} + c_0 n - E_p}}{\sqrt{2E_p}} \hat{a}^\dagger_{-\mathbf{k},0},$$

$$\hat{b}_{\mathbf{k},\pm} = \frac{\sqrt{\epsilon_{\mathbf{k}} + q + c_1 n + \xi_{\mathbf{k}}}}{\sqrt{2\xi_{\mathbf{k}}}} \hat{a}_{\mathbf{k},\pm 1} - \frac{\sqrt{\epsilon_{\mathbf{k}} + q + c_1 n - \xi_{\mathbf{k}}}}{\sqrt{2\xi_{\mathbf{k}}}} \hat{a}^\dagger_{-\mathbf{k},\mp 1}. \tag{B10}$$

The first mode E_p in Eq. (B9) is a phonon mode. The other two are magnon modes which scatter a quasiparticle from the state with $m=0$ to the one with $m=\pm 1$. Thus, in this phase as in the ferromagnetic phase, phonons and magnons are decoupled.

[1] D. M. Stamper-Kurn, M. R. Andrews, A. P. Chikkatur, S. Inouye, H.-J. Miesner, J. Stenger, and W. Ketterle, Phys. Rev. Lett. **80**, 2027 (1998).
[2] J. Stenger, S. Inouye, D. M. Stamper-Kurn, H.-J. Miesner, A. P. Chikkatur, and W. Ketterle, Nature (London) **396**, 345 (1998).
[3] H.-J. Miesner, D. M. Stamper-Kurn, J. Stenger, S. Inouye, A. P. Chikkatur, and W. Ketterle, Phys. Rev. Lett. **82**, 2228 (1999).
[4] D. M. Stamper-Kurn, H.-J. Miesner, A. P. Chikkatur, S. Inouye, J. Stenger, and W. Ketterle, Phys. Rev. Lett. **83**, 661 (1999).
[5] A. Görlitz, T. L. Gustavson, A. E. Leanhardt, R. Löw, A. P. Chikkatur, S. Gupta, S. Inouye, D. E. Pritchard, and W. Ketterle, Phys. Rev. Lett. **90**, 090401 (2003).
[6] H. Schmaljohann, M. Erhard, J. Krönjager, M. Kottke, S. van Staa, L. Cacciapuoti, J. J. Arlt, K. Bongs, and K. Sengstock, Phys. Rev. Lett. **92**, 040402 (2004).
[7] M.-S. Chang, C. D. Hamley, M. D. Barrett, J. A. Sauer, K. M. Fortier, W. Zhang, L. You, and M. S. Chapman, Phys. Rev. Lett. **92**, 140403 (2004).
[8] T. Kuwamoto, K. Araki, T. Eno, and T. Hirano, Phys. Rev. A **69**, 063604 (2004).
[9] T.-L. Ho, Phys. Rev. Lett. **81**, 742 (1998).
[10] T. Ohmi and K. Machida, J. Phys. Soc. Jpn. **67**, 1822 (1998).
[11] C. V. Ciobanu, S. K. Yip, and T.-L. Ho, Phys. Rev. A **61**, 033607 (2000).
[12] M. Ueda and M. Koashi, Phys. Rev. A **65**, 063602 (2002).
[13] C. K. Law, H. Pu, and N. P. Bigelow, Phys. Rev. Lett. **81**, 5257 (1998).
[14] M. Koashi and M. Ueda, Phys. Rev. Lett. **84**, 1066 (2000).
[15] T.-L. Ho and S. K. Yip, Phys. Rev. Lett. **84**, 4031 (2000).
[16] W.-J. Huang and S.-C. Gou, Phys. Rev. A **59**, 4608 (1999).
[17] M. Ueda, Phys. Rev. A **63**, 013601 (2000).
[18] P. Szépfalusy and G. Szirmai, Phys. Rev. A **65**, 043602 (2002).
[19] L. E. Sadler, J. M. Higbie, S. R. Leslie, M. Vengalattore, and D. M. Stamper-Kurn, Nature (London) **443**, 312 (2006).
[20] N. N. Klausen, J. L. Bohn, and C. H. Greene, Phys. Rev. A **64**, 053602 (2001).
[21] E. G. M. van Kempen, S. J. J. M. F. Kokkelmans, D. J. Heinzen, and B. J. Verhaar, Phys. Rev. Lett. **88**, 093201 (2002).
[22] J. Goldstone, Nuovo Cimento **19**, 154 (1961).
[23] N. N. Bogoliubov, J. Phys. (USSR) **11**, 23 (1947).
[24] H. Saito and M. Ueda, Phys. Rev. A **72**, 023610 (2005).
[25] H. Saito, Y. Kawaguchi, and M. Ueda, Phys. Rev. Lett. **96**, 065302 (2006).